LIP-STUDENTS-22-09

# Probing the vaccum with di-Higgs production

Diogo Nunes[1,a] and Francisco Casalinho[1,b]

[1] *Faculdade de Ciências e Tecnologias da Universidade de Coimbra, Coimbra, Portugal*

Project supervisor: Filipe Veloso, Ricardo Gonçalo *October 18, 2022*

**Abstract.** The Higgs boson is unique among all known particles, and intimately connected to the breaking of electroweak symmetry that shaped the fundamental forces in the universe today. The study of its properties and interactions can give us invaluable clues to what new physics may be behind the Standard Model. In this internship, we studied the production of events containing two Higgs bosons, at the Future Circular Collider, a giant collider being planned at CERN to reach even higher energy than the Large Hadronic Collider. For this, we use a Monte Carlo simulation of the collisions and we analyzed the results.

KEYWORDS: Higgs, FCC, electrons, positrons, quarks and anti-quarks b

## 1 Introduction

Our current model of particle physics, the Standard Model, describes three of the four fundamental forces (Strong, Weak and Electromagnetic) classifying all currently known elementary particles. One of the elementary particles has been studied not only to have a better understanding of it but also because it is a source that may indicate the existence of new physics, the particle being the Higgs boson [1]. For a more advanced survey of this sector of the Higgs, a new infrastructure is being prepared, the Future Circular Collider, FCC [2], allowing a more precise and in-depth study of this boson, which could lead to the answer to many of the produced questions of modern physics. In our study, we intend to simulate the collision between an electron and a positron to electron, a positron and two pairs of b and anti b quarks. These b quarks come from the decay of the Higgs boson, whose decay branching ratio is 57.1% [3].

For all processes, 10000 events were generated without systematic uncertainties, in order to obtain results with an acceptable level of precision in the construction of the figures and the table, which will be presented throughout the article.

## 2 MadGraph

During the internship, we used the MadGraph software (which is a Monte Carlo event generator for collider studies) for basic simulations of particle collisions in high energy physics. We generated the electron-positron collisions producing one electron-positron, and one pair of Higgs bosons, using the Standard Model (SM). With this study we hope that our results and conclusions presented here will be promising for later in the study of Higgs physics at the FCC-ee. The implemented model, SM, is specified by a Lagrangian that contains all information about the interactions of the particles present in this model.

Programs used:

1) MadAnalysis4 is a program that allows to do physical analysis of event files;

2) Gnuplot served to plot graphs taking into account the points provided when using MadAnalysis4;

3) Delphes is a detector response simulation framework that receives as input a file of monte-carlo events and produce as output a .root file, which containg C++ objects stored on disk. These files can be opened by starting the ROOT program;

4) ROOT is designed for particle physics data analysis and contains several features specific to this field;

5) ExRootAnalysis was used to convert LHE files to ROOT format;

6) MadSpin was indispensable to cause the decay of some particles into others;

## 3 Example of how the FCC-ee will work

In the collision of one positron with one electron, producing HZ, with a given Center of Mass Energy, $E_{CM}$ ,between 220 and 800 GeV, it is possible to observe a peak at 240 GeV. This peak indicates the center of mass energy predicted by the FCC-ee [4] (approximately equal to the sum of the masses of the two bosons present after decay). The cross-section was calculated for $E_{CM}$ between 220 and 800 GeV at 10 GeV intervals, as shown in Figure 1.

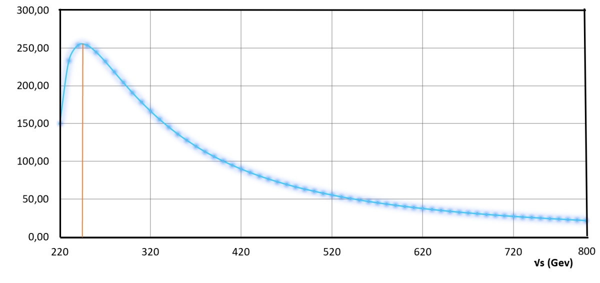


Figure 1: Z Higgs bosons production cross section as a function of $E_{CM}$

[a]e-mail: diogonuns11@outlook.pt

[b]e-mail: franciscocasalinho@icloud.com

## 4 Signal and Background

### 4.1 Signal: $\mathbf{e^+e^- \rightarrow e^+e^-hh, h \rightarrow b\bar{b}}$

The effective cross-section predictions presented below in this section are calculated with MadGraph, which generates and evaluates all possible diagrams in leading order. Figure 2 shows the Feynman diagrams for the signal, where each Higgs decays into a pair of bottom and anti-bottom quarks.

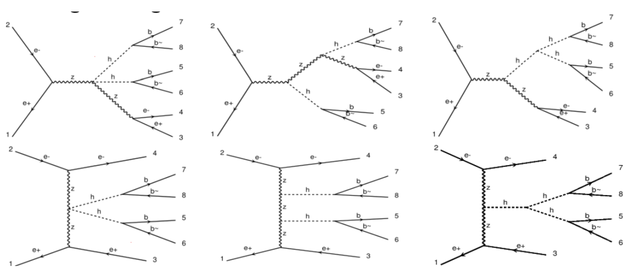

Figure 2: Signal diagrams

### 4.2 Background

The estimate of background processes is a fundamental task for FCC-ee analyses, therefore, a brief overview of background determination methods follows.
No signal diagram should be expected in background.

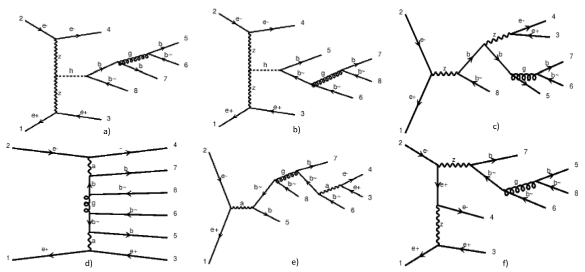

Figure 3: Background diagrams: The process $e^+ e^- \rightarrow$ h $\rightarrow e^+ e^-$ $b\bar{b}$ $b\bar{b}$ contains 16 diagrams, whose contribution is high in the background calculation, two of which are a) and b). The process $e^+ e^- \rightarrow e^+ e^-$ $b\bar{b}$ $b\bar{b}$ /h (excluding the Higgs boson as intermediate particle) contains 476 diagrams, 4 of which are c), d), e) and f).

### 4.3 Background reduction

All 592 Feynman diagrams corresponding to background had only one or no Higgs. It should be noted that the sum of the signal and background is not equal to the total, yellow color line, because there is interference and because not all background contributions can be determined with sufficient accuracy for a background estimate based solely on Monte Carlo simulations. It is easily observed graphically that the signal to noise ratio is very small, as we will show further up in the table. The process generated for the noise and for the total are illustrated in the figure 4.

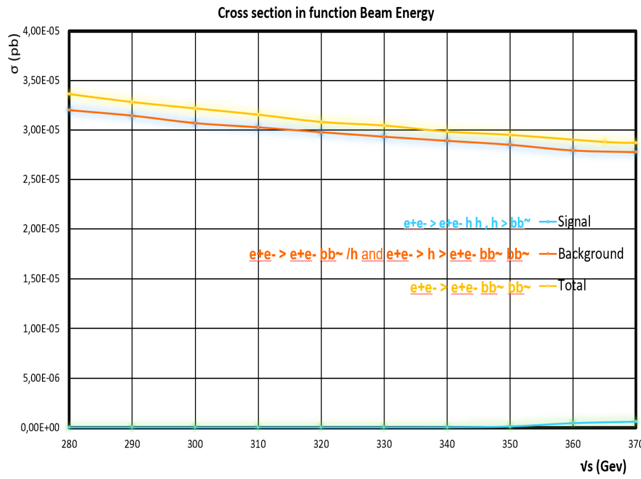


Figure 4: Relation Signal-Background

The measurement of the production of pairs of Higgs bosons is a large scale scientific project that aims to extract a tiny signal from a large background.

In the next two subsections we will show ways to improve the signal to noise ratio.

For all the cuts that we applied to the different pairs of particles resulting from the decay, the signal remained practically the same as the blue curve of the graph in the figure above.

#### 4.3.1 *PT cuts*

The background effects are sizeable, but they can be reduced by appropriate choice of cuts.

For the graph of Figure 5a: as the detector cannot detect low energy electrons, we will cut the electron energy above 20 GeV, which causes a small decrease in background compared to the previous graph. The same does not happen in the graph of Figure 5b, that when we impose a minimum energy on the $b\bar{b}$ quark pair, we cut off a large part of the background. As in the background (orange line) we produce 2 $b\bar{b}$ pairs with only 1 Higgs or none, these $b\bar{b}$ pairs can come directly from the collision between electron and positron, that is, $b\bar{b}$ quarks can be produced with a much lower energy, which when cut leads to the reduction of much of the background, in this way we start to be competitive with the signal. The background ranges from $10^{-5}$ pb to $10^{-7}$ pb for $\sqrt{s}$ = 280 GeV.

In both figures, a minimum transversal moment cut of 20 GeV was applied to the $e^+e^-$ pair and to the $b\bar{b}$ pair, in which we verified that the signal is very little affected.

In the Center of Mass Energy range from 350 GeV to 370 GeV we are already sensitive to the signal.

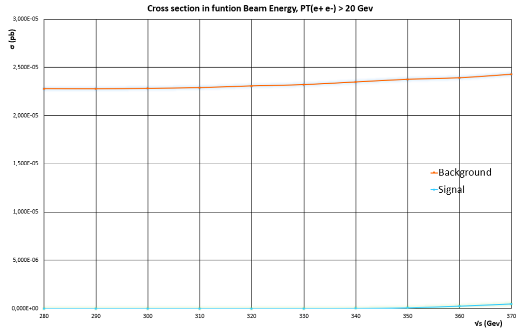


(a) min $P_T$ = 20 GeV (electrons)

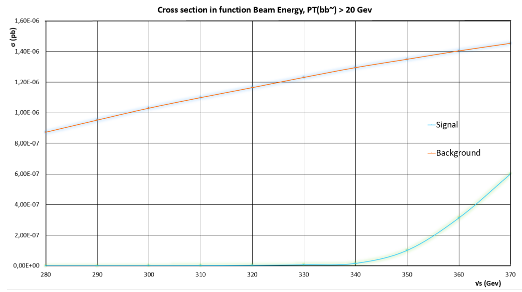


(b) min $P_T$ = 20 GeV (b-quark)

Figure 5: Transverse momentum distributions

### 4.3.2 Invariant mass of b$\bar{\text{b}}$ pairs

Signal events have Higgs bosons and then the invariant mass of the b$\bar{\text{b}}$ pairs has to give the Higgs mass, 125 GeV.

In the second figure that is the background, the peak is no longer the same because there are more diagrams in which there is production of a pair of b$\bar{\text{b}}$ from a Z boson with a mass of 91 GeV [5]. Hence the peak is close to this point, but below this value because the Z boson will radiate the second pair of b$\bar{\text{b}}$. Even so, it is said that the mass of the b$\bar{\text{b}}$ pair can be 125 GeV, but with little probability.

| | Without applying invariant mass bb | | | Invariant mass bb above 90 Gev | | | Ratio |
|---|---|---|---|---|---|---|---|
| Ecm (Gev) | Signal (pb) | Background (pb) | S/√(B) | Signal (pb) | Background (pb) | S/√(B) | S/√B improvement (%) |
| 280 | 3,414E-12 | 3,197E-05 | 6,038E-10 | 3,414E-12 | 1,020E-13 | 1,069E-05 | 99,994 |
| 290 | 5,550E-11 | 3,142E-05 | 9,901E-09 | 5,569E-11 | 4,109E-13 | 8,688E-05 | 99,989 |
| 300 | 2,906E-10 | 3,067E-05 | 5,247E-08 | 2,903E-10 | 1,392E-12 | 2,461E-04 | 99,979 |
| 320 | 2,534E-09 | 2,976E-05 | 4,645E-07 | 2,556E-09 | 7,023E-12 | 9,645E-04 | 99,952 |
| 340 | 1,519E-08 | 2,889E-05 | 2,826E-06 | 1,518E-08 | 2,291E-11 | 3,171E-03 | 99,911 |
| 370 | 6,049E-07 | 2,776E-05 | 1,148E-04 | 6,010E-07 | 9,030E-11 | 6,325E-02 | 99,818 |
| 400 | 1,557E-06 | 2,696E-05 | 2,999E-04 | 1,573E-06 | 2,581E-10 | 9,791E-02 | 99,694 |

Figure 6: Comparison between the Signal/$\sqrt{Background}$ ratios without applying cuts and Signal/$\sqrt{Background}$ with cuts above 90 GeV of the b$\bar{\text{b}}$ pair

For an invariant mass cut above 90 GeV, the background is drastically reduced, capturing almost the entire signal, as visible in the table of the Figure 6 and the red line in Figure 7.

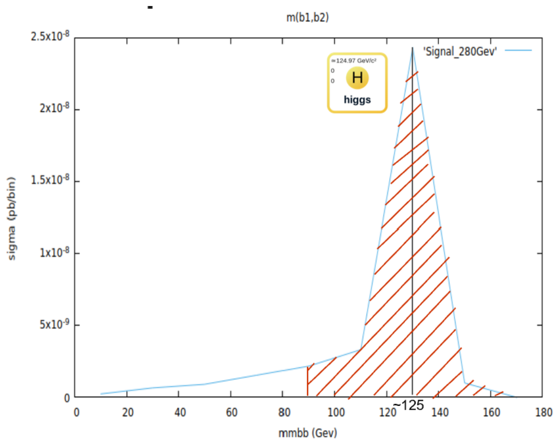


(a) Signal to $\sqrt{s}$ = 280 GeV

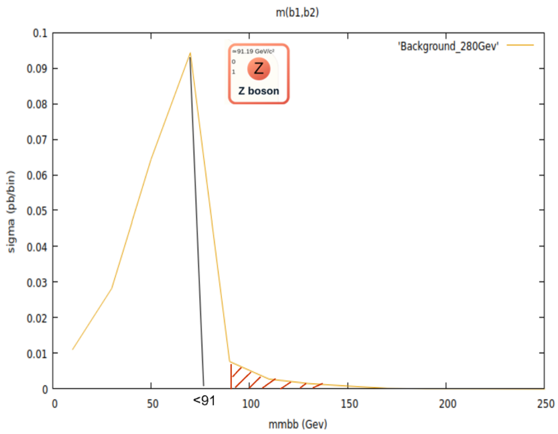


(b) Background to $\sqrt{s}$ = 280 GeV

Figure 7: Invariant Mass of the b$\bar{\text{b}}$ pair

## 5 Data Analysis

Using MadGraph, $e^+e^- \rightarrow e^+e^-$ h h events with h $\rightarrow b\bar{b}$, were generated for the following Center of Mass Energy ( $\text{E}_{CM}$ ) range from 280 to 600 GeV. for the detector simulator, Delphes was used, generating a output ROOT file, containing information about the outgoing particles generated by the process, about the jets, photons, and other parameters, all organized in classes(TTree) to be read by ROOT.

For our study, we analyzed some parameters of the following particles: electrons ($e^-$), positron ($e^+$), quark and anti-quark b, for the following $\text{E}_{CM}$: 280 and 600 GeV.

From the output file, we only use the class GenParticle, which give us the outgoing particles and with the Monte Carlo Particle Number Scheme, we choose the particles we want to study, which for our case are: ID(e∓)=±11 and ID(b/$\overline{b}$)=5/-5 [6].

Our goal for this section is the track the following properties: Energy, components of the momentum, azimuthal angle and its cosine and pseudorapidity[1].

[1] This is only for electrons and positrons

### Quarks b and $\overline{b}$

In this section, we will see the plots for b and $\overline{b}$ quarks. We will compare the results from events with 280 GeV and 600 GeV of $E_{CM}$. For the first plot,Fig.(9), we want to observe the difference in the energy range of the outgoing quarks and anti-quarks b,Fig.(9).

With the increase of the $E_{CM}$, the energy range of this outgoing particles increase as well.

To see if the particle have any preference of outgoing direction, we use the azimuthal angle for these particles, see Fig.(10).

From the Fig.(10b) and Fig.(10a), we observe that $b\overline{b}$ do not present any preferred direction.

In order to visualize the distribution of momentum of b and anti b, a two-dimensional histogram was made between momentums $P_x$ and $P_y$, Fig.(11).

Its is possible to observe that with the increase of the energy of the center of mass, from Fig.(11a) to Fig.(11b), the particles begin to taper in relation to the axis of the beam of incident particles.

### Electron and Positron

In this section we will track the outgoing electrons and positrons. However, Delphes does not differentiate between incoming and outgoing particles, so we need to impose the condition to track particles whose pseudorapiditly is less than 10, Fig(8).

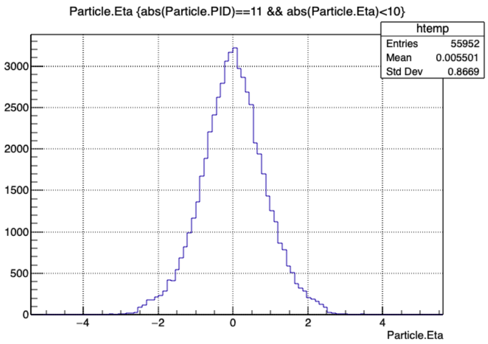


Figure 8: Pseudorapiditly

One more time, is possible to see that the the electron and positron energies increase when we change the center of mass energy from 280 GeV to 600 GeV, Fig(12).

The azimuthal angle distribution, Fig.(13), shows us that we have an isotropic distribution of these outgoing particles.

For the x and y components of the momentum, Fig.(14), we make a two-dimensional histogram, we see again that it is possible to observe that with the increase in the energy of the center of mass, the particles begin to align with the beam. It is also possible to observe a ring around the center, this could be due to the choice for pseudo-rapidity, or due to the type of process that originates these particles. Unlike quarks, these electrons and positrons can come from Z-boson decay or they can come from scattering, which creates a cone around the center.

## 6 Results and Conclusions

The objective of this work was to analyze the Higgs sector, more precisely, namely the triple Higgs coupling (Higgs decaying to two Higgs). More work is needed to perform such an analysis.
Taking into account the simulated data collected, we can say that they were as expected.

## Acknowledgments

We would like to thank our supervisors, Filipe Veloso and Ricardo Gonçalo for the immense and tireless work helping us understanding how to use MadGraph and understand some aspects of the data collected, but also for being always available to us when something wouldn't add up.
We would also like to thank LIP for the amazing opportunity they provided us by letting us see how science progression works at the frontier of human knowledge.

## References

[1] K. Jakobs et al., *The Higgs Boson discovery*, http://www.scholarpedia.org/article/The_Higgs_Boson_discovery (2015), [Online]

[2] I. Agapov, M. Benedikt, A. Blondel, M. Boscolo, O. Brunner, M.C. Llatas, T. Charles, D. Denisov, W. Fischer, E. Gianfelice-Wendt et al., *Future circular lepton collider fcc-ee: Overview and status* (2022), `https://arxiv.org/abs/2203.08310`

[3] G. Aad, , B. Abbott, J. Abdallah, O. Abdinov, R. Aben, M. Abolins, O.S. AbouZeid, H. Abramowicz, H. Abreu et al., The European Physical Journal C **76** (2016)

[4] P. Azzurri, G. Bernardi, S. Braibant, D. d'Enterria, J. Eysermans, P. Janot, A. Li, E. Perez, The European Physical Journal Plus **137** (2021)

[5] *What are Leptons? - Universe Today*, https://www.universetoday.com/46935/leptons/

[6] M. Tanabashi, K. Hagiwara, K. Hikasa, K. Nakamura, Y. Sumino, F. Takahashi, J. Tanaka, K. Agashe, G. Aielli, C. Amsler et al. (Particle Data Group), Phys. Rev. D **98**, 030001 (2018)

# Plots

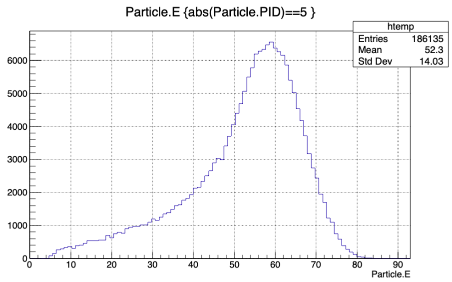


(a) $E_{CM}$=280 GeV

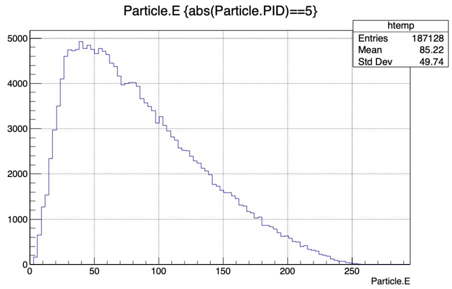


(b) $E_{CM}$=600 GeV

Figure 9: Energy, $b\bar{b}$

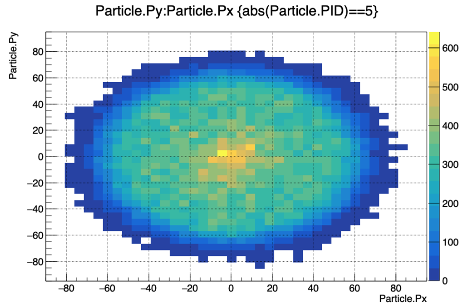


(a) $E_{CM}$=280 GeV

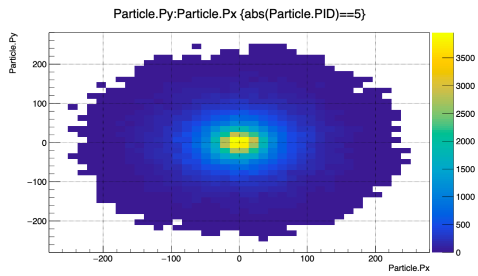


(b) $E_{CM}$=600 GeV

Figure 11: $P_y$ versus $P_x$, $b\bar{b}$

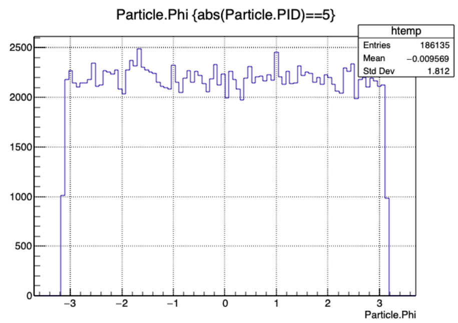


(a) $E_{CM}$=280 GeV

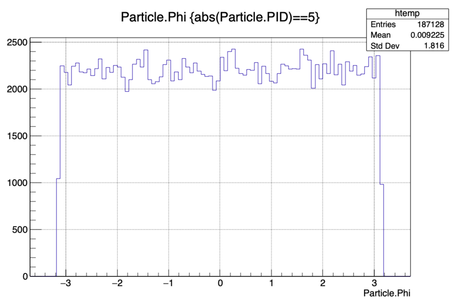


(b) $E_{CM}$=600 GeV

Figure 10: Azimuthal angle, $b\bar{b}$

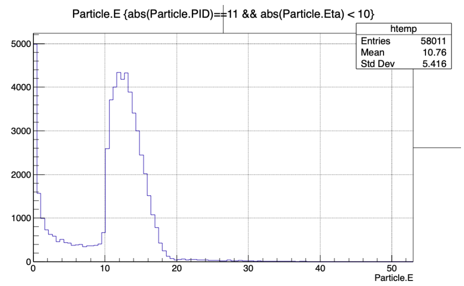


(a) $E_{CM}$=280 GeV

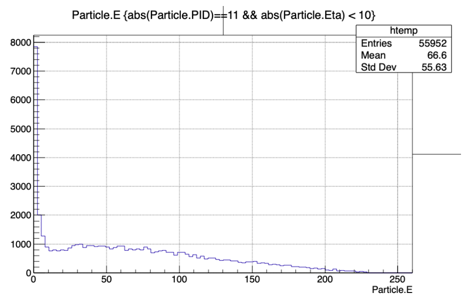


(b) $E_{CM}$=600 GeV

Figure 12: Energy, $e^-$ $e^+$

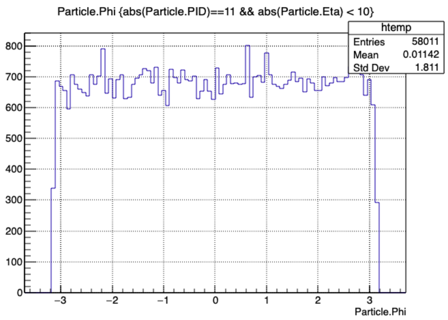


(a) $E_{CM}$=280 GeV

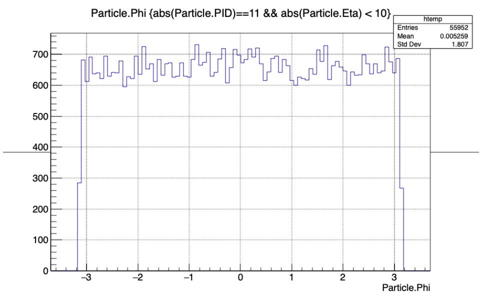


(b) $E_{CM}$=600 GeV

Figure 13: Azimuthal angle, $e^-$ $e^+$

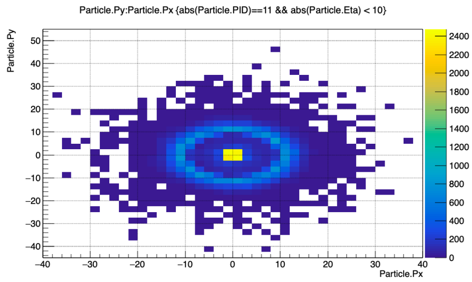


(a) $E_{CM}$=280 GeV

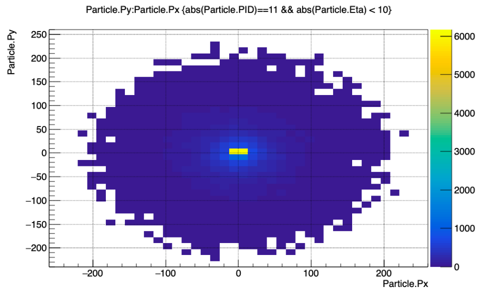


(b) $E_{CM}$=600 GeV

Figure 14: $P_y$ versus $P_x$, $e^-$ $e^+$